Turkish Journal of Civil Engineering, 2025, xxxx-xxxx, Paper xxx, ***Research Article***

Behavior of Fiber Reinforced Concrete Beams with Inadequate Torsion Steel under Pure Torsion

Yılmaz Öğünç TETİK[1*]
Osman KAYA[2]

ABSTRACT

To investigate the relationship between reinforced concrete beams under pure torsion and steel fiber usage, 16 large-scaled reinforced concrete beams with inadequate torsion steel were designed and produced. For experiments, a new test setup was designed to allow specimens to have rotational movement on one end and axial movement on the other end. The variables were selected as 300 and 400 mm spacings of transverse reinforcements and 0.0%, 0.3%, 0.6%, 0.9%, 1.2%, and 1.5% by volume of the mixture as steel fiber ratios. Cracking torque, maximum torque and ultimate torque values were obtained experimentally, and torque-twist curves and energy dissipation capacities were determined. Findings were compared to indicate the relationship between variables. Results showed that certain values of steel fiber ratio as a replacement material for relevant spacing of transverse reinforcements.

Keywords: Reinforced concrete beam, pure torsional moment, steel fiber, energy dissipation capacity.

1. INTRODUCTION

Flexural moments and shear forces are primary considerations in the design of reinforced concrete (RC) beams. Although pure torsion rarely occurs in RC beams, the behavior of elements under pure torsion needs to be defined explicitly to understand their overall combined flexural and torsional response [1]. It is known that plain concrete beams under torsional loading typically fail in a brittle manner once tensile stresses exceed the concrete's tensile strength limit. In torsional behavior, reinforcement contributes after the cracking, and it provides gaining more ductile behavior. It is highlighted that reinforcement begins to

Note:
- This paper was received on September 11, 2023 and accepted for publication by the Editorial Board on November, 15, 2024.
- Discussions on this paper will be accepted by xxxxxxx xx, xxxx.

• https://doi.org/10.18400/tjce.1358643

1 Muğla Sıtkı Koçman University, Department of Civil Engineering, Muğla, Türkiye
yilmazogunctetik@mu.edu.tr - https://orcid.org/0000-0002-0104-1555

2 Muğla Sıtkı Koçman University, Department of Civil Engineering, Muğla, Türkiye
osmankaya@mu.edu.tr - https://orcid.org/0000-0003-3851-3082

* Corresponding author

contribute to more ductile behavior after cracking, significantly influencing the torsional capacity of RC beams [2].

The researchers examined various factors affecting torsional behavior. The ratios of transverse and longitudinal reinforcement, known as the torsional reinforcement ratio, play a critical role [3], where excessive reinforcement can reduce torsional ductility [4]. Also, it is reported that the aspect ratio of the beam cross-section [5,6] and the compressive strength of the concrete have a considerable impact on designing [7]. Additional studies have observed that increases in compressive strength beyond a certain threshold led to decreased twist angles and reduced ductility [8,9].

Steel fibers (SF) have been shown to enhance the crack resistance in reinforced concrete (RC) beams. SF contributes to a pseudo-ductile tensile response by transferring tensile stress across cracks and offering significant shear resistance [10]. It is also known that using steel fibers as shear reinforcements provides efficient ductility on RC beams [11]. Earlier experimental studies showed that concrete beams reinforced with steel fiber exhibit improved torsional strength [12]. When the behavior of plain concrete members reinforced with steel fibers was examined, it was observed that an increased steel fiber ratio provides greater torque capacity and enhances the first cracking load of the beam under pure torsion [13]. In other aspects, SF with a high-volume fraction in high-strength concrete (HSC) was revealed to have a more ductile form [14]. Moreover, SF also enhances the ultimate torsional strength and torsional stiffness after the initial cracking, particularly in ultra-high-performance beams [15]. Besides, the impact of different types of steel fiber on ductility and toughness was also examined. Double-hooked and kinked steel fibers increased the flexural tensile strength of the beams at the maximum level [16]. Additionally, the effects of the SF ratio and the aspect ratio of SF on the behavior of reinforced concrete (RC) beams under torsional moments were investigated. It is seen that the torsional strength of the beams was enhanced in a 0.6% volumetric ratio with an amount of 10–60% [17,18].

Recent research has extended into exploring the behavior of various beam shapes under torsion, including not only traditional rectangular or circular beams [19] but also T and L-shaped beams [20]. In the experimental study that considered only longitudinal reinforcement, it was observed that the ductility capacity of steel fiber-reinforced rectangular beams was higher than that of the corresponding flanged beams [21].

In experimental studies, researchers preferred ACI318 [22], EC2 [23], CSA [24] and JSCE [25] standards for designing the beams [3,6]. However, mostly, these standards' torsional design equations are generated by shear design and the modified forms of it. To determine the strength of SFRC beams under pure torsional loading, a model was developed by comparing 23 test results [26]. An empirical equation was proposed for estimating the torsional capacity of rectangular RC beams [27]. Also, the space truss analogy was modified to find the bearing capacities of the RC beams under pure torsion [28]. A simplified torsional strength model for SFRC beams was proposed based on the softened truss model and validated by test data obtained from the literature [29].

Despite experimental and analytic investigations displaying valuable results, the area is still open for new findings and suggestions. This paper examines the behavior of RC beams designed according to the provisions of the Turkish Standard TS 500 [30]. The novelty of this experimental study consists of determining the behavior of beams designed under TS500,

which have been strengthened with steel fibers. The study focuses on identifying an optimal steel fiber ratio as a potential replacement material for determined transverse reinforcement spacings. In the experimental study, 16 beams were tested for constant cross-sections. Volumetrically, five different steel fiber ratios and also two different stirrup spacings were selected as parameters. To find the relationship between steel fiber and transverse reinforcement, torsional moments were determined. The torque-twist curves and energy dissipation curves were obtained based on the test results and findings were compared.

2. EXPERIMENTAL STUDY

2.1. Materials

To obtain identical concrete strength, ready-mixed concrete with 35 MPa characteristic strength was selected in the production stage of the specimens. During the casting process, ten cylindrical samples with the size of 100x200 mm were taken from the concrete with and without steel fibers. These samples were tested to determine the compressive strength of the concrete on the day when the experiments were conducted. The test results of the samples are given in Table 1. For all specimens, 12 mm diameter rebars and 8 mm diameter rebars were used as longitudinal and transverse reinforcements, respectively. The average yield strength of both transverse and longitudinal reinforcement is found to be 583 and 506 MPa, respectively.

Table 1 - Compressive strengths of 100x200 samples

Fiber content (%)	Compressive strength (MPa)
0.0	36.41
0.0	30.95
0.0	37.35
0.0	29.04
0.0	48.22
0.3	43.07
0.6	30.85
0.9	36.06
1.2	36.56
1.5	36.08

The two-sided bent-ended Kemerix® 80/60 BG steel fiber used in the concrete is shown in Figure 1. The chosen fiber had an aspect ratio (l_f/d_f) of 80, length of 60 mm, and 0.75 mm diameter (Fibers were supplied by Kemerli Metal Pty Ltd., Turkey: used as a substitute for the known counterpart Dramix®). While l_f represents the length, d_f symbolizes the diameter of steel fibers. The average yield strength of the steel fiber was f_{yf} = 1200 MPa, which was taken from the manufacturer's datasheet.

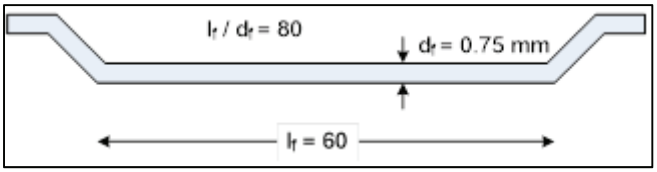

Figure 1 - Geometry of steel fibers

2.2. Specimen Details

The test specimens were designed according to the requirements defined in Turkish Standard TS500 [30]; however, the standard lacks a specification regarding pure torsion. To prevent brittle failure, Eq. 8.17 of TS500 is suggested. The requirements given in the standard are entirely related to combined torsion and shear forces. In most equations, a shear term is needed to get the results. However, the shear force should not be considered when designing the specimen for pure torsion. To meet the requirements and avoid the incalculability of the equations, the design shear force (V_d) was assumed as 1 N in this study.

The mechanical properties of 16 beams produced in total were 300x300 mm in cross-sectional area and 2000 mm in length. 4Φ12 rebars were used as longitudinal reinforcements in all specimens. The dimensions of the test specimens and reinforcement layout are given in Figure 2. The specimens were designed with 300 mm and 400 mm stirrup spacings in the test regions. One of the main objectives of this study is to explore the effects of steel fibers on torsional behavior. For this reason, two different transverse reinforcement ratios, both less than the requirements defined in section 8.2.6 of the TS 500 standard, were selected. Therefore, as Table 2 shows, 8 specimens were produced with 300 mm spaced stirrups, and the remaining 8 were produced with 400 mm spaced stirrups. To prevent premature failure at the supports, a high amount of transverse reinforcement was used in these regions.

Another parameter was the volumetric fraction (V_f) of steel fibers. Many fiber aspect ratio variations are preferred according to beam type and its cross-section in previous studies [21, 31, 32,33]. Besides, loss of compressive strength and tensile toughness can be observed in high fiber ratios in beams [34, 35]. To determine a specific volume fraction, fiber ratios were chosen as 0.3%, 0.6%, 0.9%, 1.2%, and 1.5% volumetrically. The corresponding weight values and fiber contents were approximately determined as 4.2, 8.5, 12.7, 16.9, and 21.1 kg, respectively. It should also be considered that high fiber content might cause significant problems in casting operations especially if concrete composition is not well designed and controlled on-site. Essential attention was paid to preventing the formation of fiber balls in the mix and avoiding workability problems.

As for the designation of the specimens in this test, *s* indicated the spacing of transverse reinforcements in the test region, and V indicated the volume fraction of the steel fiber. When the 'V' block was null, it specified the specimens without steel fibers. Three identical specimens called I, II, and III were produced as non-fibrous specimens for both 300 mm and 400 mm stirrup spacings. The classification of each specimen including all parameters is detailed in Table 2.

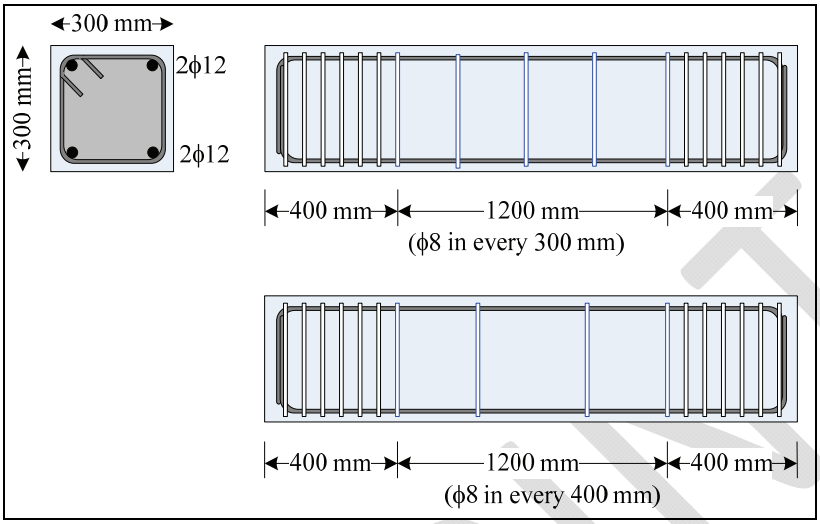

Figure 2 - Dimensions of test specimens and reinforcement details

Table 2 - Nomenclature and properties of specimens

Beam Designation	Φ8 transverse reinforcement spacing (cm)	Fiber volume fraction (%)
S30V00- I	30	**0**
S40V00- I	40	**0**
S30V00- II	30	**0**
S40V00- II	40	**0**
S30V00- III	30	**0**
S40V00- III	40	**0**
S30V03	30	**0.3**
S40V03	40	**0.3**
S30V06	30	**0.6**
S40V06	40	**0.6**
S30V09	30	**0.9**
S40V09	40	**0.9**
S30V12	30	**1.2**
S40V12	40	**1.2**
S30V15	30	**1.5**
S40V15	40	**1.5**

2.3. Test Setup and Instrumentation

The schematic depiction of the produced test setup is given in Figure 3 with frontal (a) and side (b) views. Unlike more conventional methods [36,37], the load was applied by a hydraulic pump (actuator) from endpoints with a 100 kN capacity in tension and

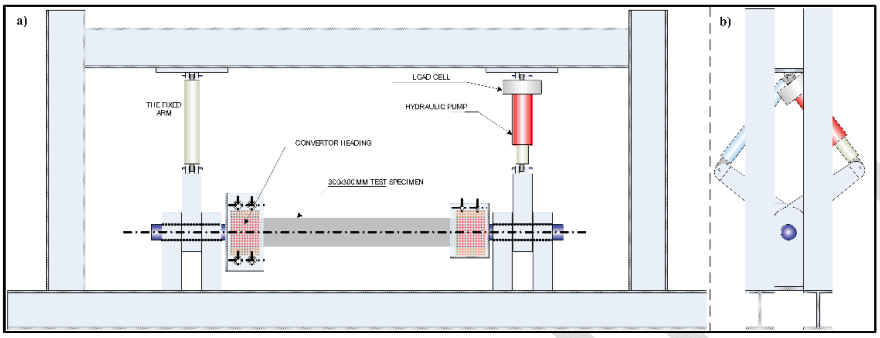

Figure 3 - Design of the test setup

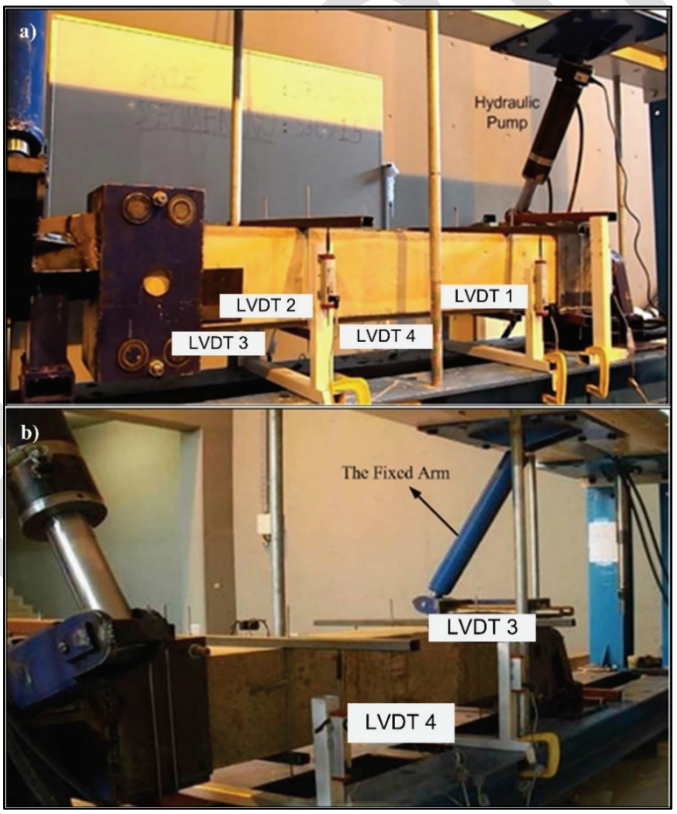

Figure 4 - The test setup, loading, and measurement systems (a) the backside of the setup (b)

compression. The load was measured by the 200 kN capacity load cell mounted on the pump. The test specimen was located inside the test setup which involved specific support conditions. The force was applied by a rigid moment arm connected to the free support. The moment arm transferred the load to the RC beam as a pure torsional moment. To determine the twisting angle in the test region, four Linear Variable Displacement Transducers (LVDT) were placed in total on the front and back sides of the beam, as shown in Figures 4a and 4b. One end was fixed rotationally but free in the axial direction with the help of rollers inside the support to allow axial elongation. The other end was free to rotate. The side view of the test setup which is positioned during an experiment is shown in Figure 5a. Also, it is depicted that rollers were placed inside the fixed support headpiece. For the elongation, on the fixed headpiece, a gap of approximately 5 cm is maintained between the outer face of the specimen and the inner plate, as shown in Figure 5b and 5c. Due to the gap and roller inside the support head, the axial resistant force becomes zero, allowing the specimen to elongate freely. The applied force is transferred to the specimen axis via the head support, which is restricted in the shear direction but free to rotate. Therefore, the specimen is not subjected to shear forces.

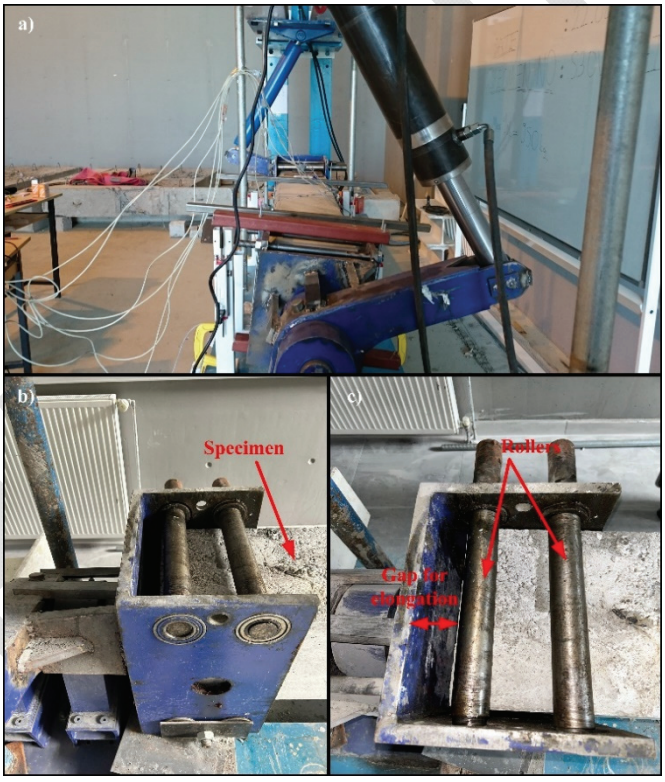

Figure 5 - a) The side view of the test setup, b) Specimen in the headpiece, c) Details of the headpiece of the test setup for elongation

The load was progressively applied at a low rate, and the data from the LVDTs and loadcell were recorded every second by the data logger. L1 to L4 are the displacement readings from

the test region and D1 and D2 are the clear horizontal lengths between the LVDTs (Figure 6a). The calculation of rotation (θ) for each end of the test region is depicted in Figure 6b and given in Eq. 1. Additionally, the angle of twist (φ) in the test region is calculated from Eq. 2.

$$\tan(\theta_i) = \frac{L_1+L_4}{D_1} \quad \text{and} \quad \tan(\theta_j) = \left(\frac{L_2+L_3}{D_2}\right) \tag{1}$$

$$\tan(\varphi) = \frac{(\theta_j)-(\theta_i)}{\ell_{average}} \tag{2}$$

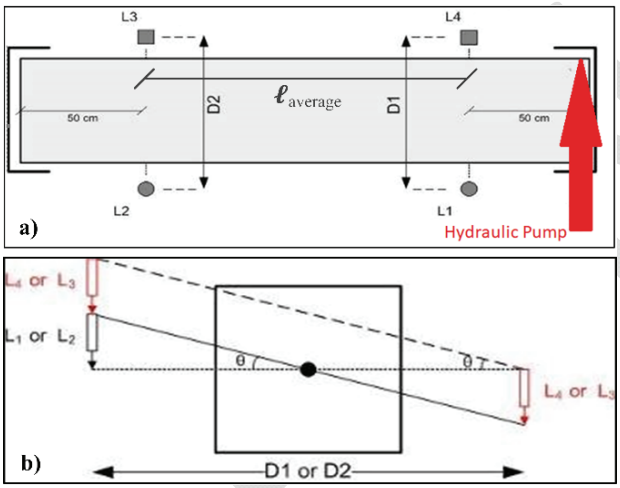

Figure 6 - Locations of LVDTs (a) rotation calculations (b)

As evident in literature data, smeared crack analysis is used for a rational estimation of torsional strengths and the elastic behavior of plain concrete members. However, the present study focuses only on experimental results of plain concrete as a reference point for the comparison of steel fiber-reinforced concrete's torsional values with the angle of twist [38].

3. TEST RESULTS AND DISCUSSION

Due to difficulties encountered in code interpretation, specimens were designed with inadequate torsion reinforcement, leading to ultimate torsion capacity lower than the cracking capacity. Consequently, a ductile torsion behavior could not be achieved. The discussion below is therefore restricted to non-ductile torsion behavior. Derived from the test results, the cracking torque (T_{cr}), maximum torque (T_{max}), and ultimate torque (T_u) values of each specimen are shown in Table 3 along with their corresponding angle of twist values (Φ_{cr}, Φ_{max} and Φ_u). Since the specimens without SF are similar in the experiments, only the test results of S30V00-I and S40V00-I are shown. The cracking, maximum, and ultimate torques indicate the torque value when the crack formed, the maximum resistance value (considered as the peak point) was achieved, and reinforcement was ruptured, respectively. It is known that the cracking strength of fibrous reinforced concrete depends only on the strength of the

concrete matrix. It is observed that after the first crack developed in the experiments, the bearing capacity of the beams continued to increase until it reached the peak and then started to decrease. Before reaching the T_u and experiencing a sudden decrease in torque capacity, beams demonstrated a post-cracking behavior. Also, it is observed that beams demonstrated a pseudo-ductile response through fibers, proceeding with energy absorption after the reinforcements separated. Therefore, the loading was sustained in accordance with the maximum twisting capacity of the test device, and it is observed that the twisting behavior of the beams is continued.

Table 3 - Obtained test values

Beam Designation	Φ_{cr} (rad/m) ($*10^{-3}$)	T_{cr} (kNm)	Φ_{max} (rad/m) ($*10^{-3}$)	T_{max} (kNm)	Φ_u (rad/m) ($*10^{-3}$)	T_u (kNm)	Φ_u/Φ_{cr}
S30V00	0.29	3.69	1.24	3.93	38.54	3.28	132.89
S30V03	0.61	3.22	1.80	3.69	73.55	2.95	120.57
S30V06	0.81	3.89	2.94	4.15	88.79	3.32	109.61
S30V09	0.66	3.93	1.93	4.22	85.67	3.38	129.80
S30V12	0.39	3.83	1.65	4.04	64.93	3.23	166.48
S30V15	0.94	3.39	1.75	3.71	154.10	2.97	163.93
S40V00	0.30	3.19	1.52	4.05	43.24	3.37	144.13
S40V03	0.51	3.48	1.60	4.00	57.78	3.20	113.29
S40V06	0.67	3.56	1.23	3.74	74.54	2.99	111.25
S40V09	0.44	3.40	1.57	3.75	59.47	3.00	135.15
S40V12	0.59	3.92	1.46	4.36	72.06	3.49	121.13
S40V15	0.68	3.54	2.01	4.06	56.20	3.25	82.67

The final twist value depends on the specimen twist capacity or actuator stroke capacity. This causes variation in ultimate twist and torque values. To be consistent, it is assumed that the failure of the specimen was developed when the torque was dropped by 20% of T_{max} (T_u=0.80*T_{max}). In Table 3, the ultimate torque and corresponding twist were given.

Regardless of fiber or steel content, the first cracking twist depends on the concrete type. As seen from Table 3, the maximum torques of specimens were low for low fiber contents and it is low again for higher fiber content for S30 and S40 groups. For the S30 group, the decrease in T_{max} started after 0.9% fiber content, and it started after 1.2% fiber content for the S40 group. Figure 7 shows the Φ_u/Φ_{cr} ratios–variation concerning the fiber content. The Φ_u/Φ_{cr} ratios are almost same for lower fiber content for both S30 and S40 groups. However, the variation dispersed as the fiber content exceeds 9%. For S40 specimens, the Φ_u/Φ_{cr} ratios getting less for higher SF contents. In this case, fibers might create weak points or reduce certain properties of the concrete due to the interaction between the steel fibers and the concrete matrix.

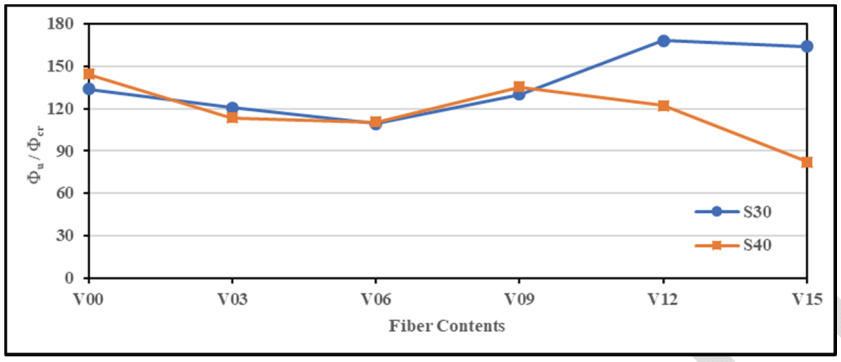

Figure 7 - Variation of Φ_u/Φ_{cr} ratios for S30 and S40 specimens' group

- In experiments, after the first crack was observed, the torsional moment continued to increase. It is also observed that number of cracks in steel fibrous beams was significantly higher than in non-fibrous ones. In the non-fibrous beam tests, a few torsional diagonal cracks occurred, and with an increase in the load level, these cracks were propagated and widened. Due to generated local fractures, the beams are suddenly broke. However, in fibrous beam tests, the cracks dispersed across all test regions, causing a pseudo-ductile behavior. Figure 8a and 8b show the typical crack patterns of beams without fiber (i) with moderate fiber (ii), and with an excessive fiber (iii) that are subjected to 300 mm and 400 mm spacing, respectively.

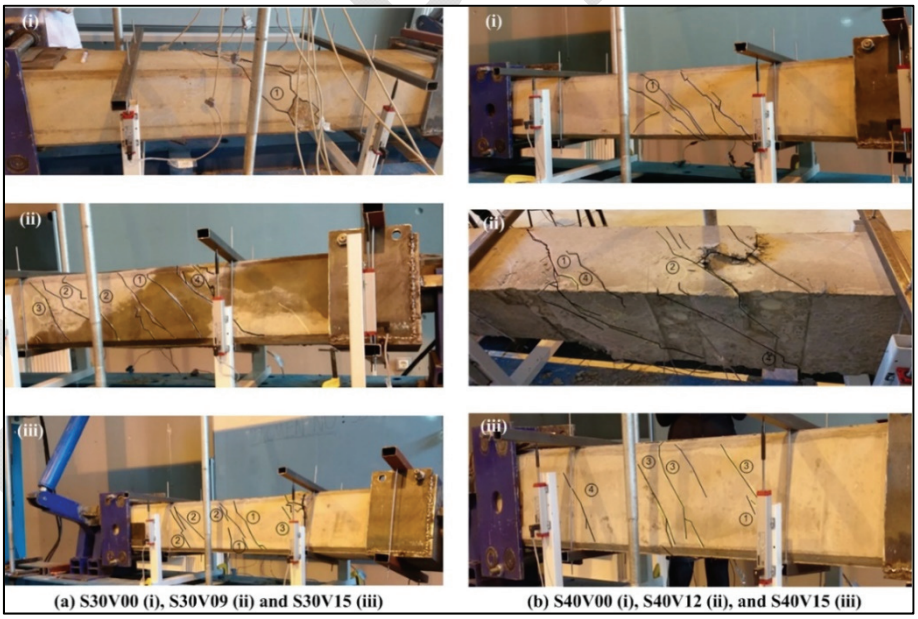

Figure 8 - Crack patterns

- The experimental results illustrate that S30 group beams predominantly displayed initial cracks within a load range of 6 kN to 7.28 kN, with beams S30V06, S30V09, and S30V12 notably demonstrating initial cracks at loads exceeding 7 kN, indicative of higher load capacities within this sub-set. For the S30V15, the first crack appeared at a 6.05 kN load and following cracks formed within very small intervals and continued to form until the maximum load was reached. The specimen failed from a point between the first and second crack. Similarly, the S40 group beams revealed initial cracks ranging from 5.94 kN to 7.28 kN, with S40V12 exhibiting the highest load resistance at 7.28 kN, reflecting the upper limit observed in this group. The first three cracks developed at 7.19, 7.22, and 7.28 kN, load respectively. The crack patterns of the S30V15 and S40V12 beams are also depicted in Figure 9a and 9b.

Figure 9 - Crack pattern of S30V15 (a) and S40V12 (b) beams

- The post-cracking response of the beams continued up to a certain volume fraction of steel fiber. However, beams with relatively high amounts of SF behaved poor twisting ability during the testing. Due to SFs displaying a bonding effect on the cracks, similar to stitches (Figure 10), the dispersing of the beams became difficult. It is proven that a high SF amount did not always increase the twisting angle due to the increased stiffness of the beams.

Figure 10 - SFs prevent the cracks

- During the testing of the beams, a disassociation was observed in transverse reinforcements. The rupture in the S30V09 beam is shown in Figure 11.

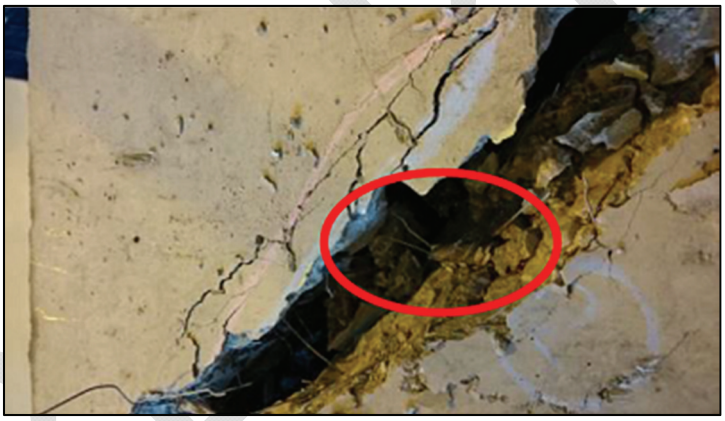

Figure 11 - The rupture of transverse reinforcement (S30V09 beam)

- The reason for observing a rupture in the stirrup was the excessive use of SF. The intense utilization SFs might have caused the reinforcements to yield more than the estimated value. Consequently, the stirrup could no longer resist and ruptured at its weakest point. To state the findings clearly, the torque-twist curves are illustrated for the beams S30V12 and S40V15, respectively in Figure 12a and 12b. The stirrups of S30V12 and S40V15 ruptured at around 79.44×10^{-3} and 90.04×10^{-3} rad/m twist levels, respectively. As shown in the diagrams, the rupture of the stirrup caused a sudden decrease in torque and presented deformations due to the angle of twist.
- It was also observed that the twisting behavior of the beams continued even after the rupture of transverse reinforcement. Although the torque values are decreased, the

bearing capacity of the beams persists because SFs resist to keep the beam block together. At this point, however, it was unexpected for the beams to display a pseudo ductility manner even after the rupture, similar to post-cracking behavior.

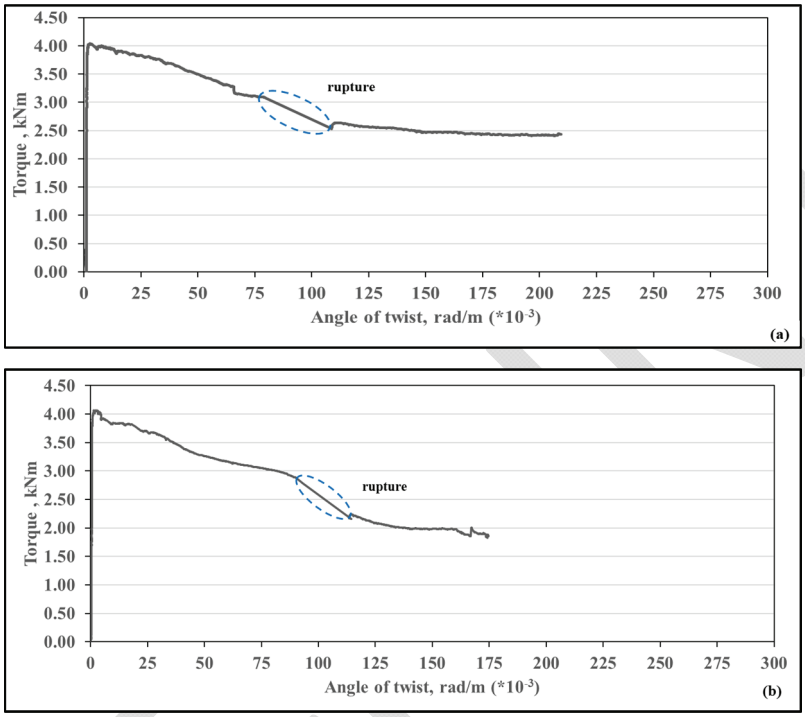

Figure 12 - Torque-twist curves of S30V12 (a) and S40V15 (b) beam

3.1. Comparison of Torque- Twist Curves and Energy Dissipation Capacities

To find out the similarity and discrepancy between the beams, the curves obtained from experiments were compared according to their twisting angles and energy dissipation capacities (EDC) under torsional loading.

The comparison of the torque-twist curves for the entire S30 group of experimental testing beams is illustrated in Figure 13a. Among them, beam S30V09 was clearly the most reasonable option for steel fiber utilization due to it reaching the maximum torque capacity. The torque-twist curve of the S40 group of testing beams is also shown in Figure 13b. As the figure summarizes, beam S40V12 was the most logical selection of all.

For better seismic performance in structural systems, a high energy dissipation capacity (EDC) in RC beams is desirable. According to the determined test results, the torsional EDCs of all beams were calculated by using the area under the torque–twist curves. Figure 14a and 14b indicate the respective cumulative EDCs of beams that have 300 mm and 400 mm transverse reinforcement spacings. The maximum EDCs of the beams and corresponding twist results are summarized in Table 4.

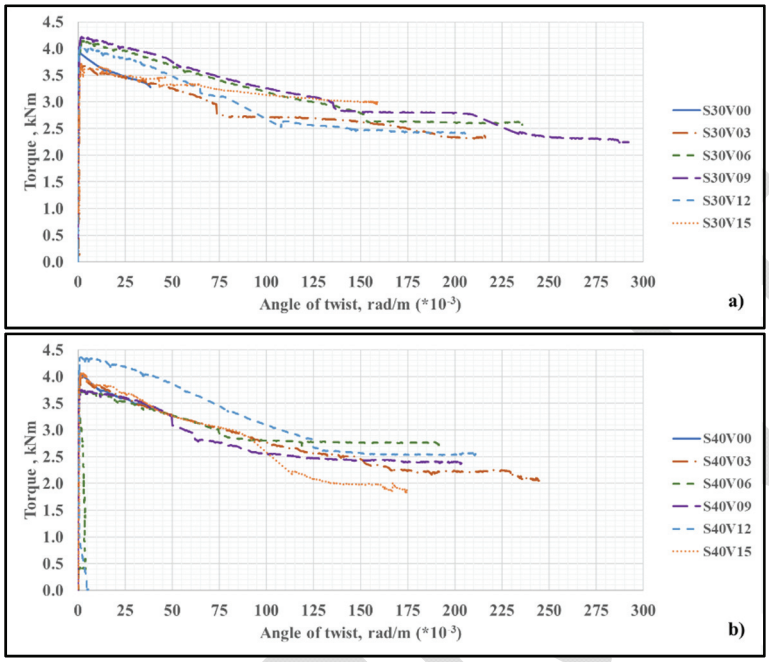

Figure 13 - Torque-twist curves of S30(a) and S40(b) group beams

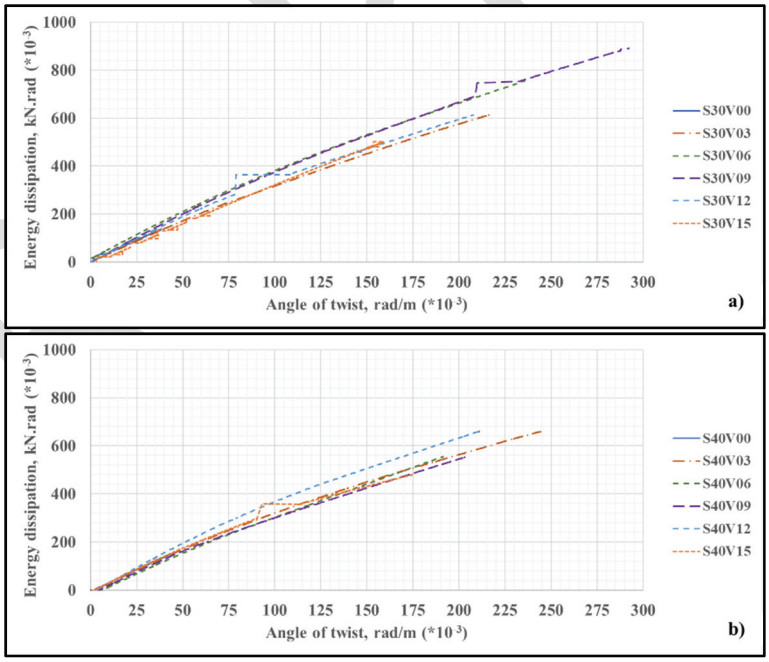

Figure 14 - Comparison of energy dissipation capacity: (a) S30 group beams and (b) S40 group beams

Table 4 - Comparison of the energy dissipation capacities of all fibrous beams

Beam designation	Maximum energy dissipation capacity, kNrad ($*10^{-3}$)	Angle of twist, rad/m ($*10^{-3}$)
S30V03	612	216.74
S40V03	668	244.35
S30V06	754	241.77
S40V06	575	190.05
S30V09	890	292.64
S40V09	566	202.98
S30V12	614	210.09
S40V12	6.60	207.76
S30V15	5.23	168.87
S40V15	4.89	174.77

Since the EDCs of the non-fibrous beams were almost identical, it is considered unnecessary to exhibit in Table 4. It was observed that the beams S30V00 and S40V00 exhibited slight twisting which corresponded to $38.65*10^{-3}$ and $43.27 *10^{-3}$ rad/m respectively, with corresponding EDCs $1.36*10^{3}$ and $1.41 *10^{3}$ kNrad. To compare the EDCs of the beams, a limit value can be determined. For instance, the EDCs were almost the same for beams S30V03 and S40V03 in $150*10^{-3}$ rad/m twisting values. It is also seen that the maximum capacity for energy dissipation of the beam S40V03 was slightly higher than that of the S30V03 beam.

Contrary to expectations, the maximum energy capacities and dissipated energies at a $150*10^{-3}$ rad/m limit value for specimens S30V12 and S40V12 were distinctive. The EDC of the S40V12 beam was higher than that of the S30V12 beam, both limit level and maximum capacity. The reason for less energy dissipation may have been due to the stirrup rupturing.

Except for beams S30V12 and S40V12, the energy dissipation capacities of all other beams in the S30 group were greater than those of their counterparts, both at the determined limit value and at maximum capacity.

4. CONCLUSION

In this study, the behavior of steel fibrous reinforced concrete beams under pure torsional moment was investigated experimentally. 16 large-scaled reinforced concrete beams with inadequate torsion steel were designed and produced. Different transverse reinforcement ratios (based on the 300 and 400 mm spacing of the closed stirrups) and SF volume fractions (0.0%, 0.3%, 0.6%, 0.9%, 1.2%, and 1.5%) were selected as parameters. Torsional moments at cracking, maximum and ultimate values along with the corresponding angle of twist behavioral curves were presented. Additionally, Φ_u/Φ_{cr} ratios of beams were given. Energy

dissipation capacities (EDCs) were also examined to validate the corresponded torque capacities of beams and to describe the relationship of torque-twist values. The determination of specific SF ratios for two different transverse reinforcement spacing can be also regarded as the novelty of this experimental study.

Based on the test results, the following findings were drawn:

- For all types of beams, up to the first cracking, the torque twist behavior was identical and can be accepted as linearly elastic. A similar situation was also seen in other studies [26].
- As expected, failure in non-fibrous beams was due to a single crack in the test region, whereas many cracks spread out in fibrous beams, with the fibers tending to restrict these cracks and improve the twisting capacity of the beams. This has been observed in similar studies [18].
- It is concluded that torque-twist responses of beams clearly showed a pronounced softening behavior after cracking, however, higher amounts of SF increased stiffness and early cracking behavior in RC beams under pure torsional moment.
- Despite the larger distance in the spacing of the stirrups in an S40 group of RC beams, the maximum torque capacities were enhanced in 1.2% and 1.5% ratios of SF. This phenomenon can be explained by the SF behavior, which was similar to that of stirrups, especially at these intense levels. The usage of SF showed a similar effect to the usage of torsional reinforcement in another study [39].
- In 0.6% and 0.9% SF ratios, the maximum EDC of the S30 group of RC beams is higher than that of the S40 group.
- EDC results showed that a certain amount of SF provides better twist capacity to beams. However, beams with SF ratios of under 0.3% and over 1.2% exhibited more rigid behavior. It is suggested by this experimental study that the implementation of SF in certain rations in RC beams results in greater EDCs under pure torsion.
- Test results showed that according to the T_{max} and determined EDCs, 0.9% and 1.2% volumetric ratios of SF were considered as the optimum value for the S30 and S40 group of RC beams, respectively. Besides, a high steel fiber amount (1.2% and 1.5%) caused less twist capacity in those groups.

In future studies, experiments can be conducted with different parameter preferences such as longitudinal reinforcement and variations in cross-section. Additionally, the range of the SF ratios could be increased, and more detailed results can be obtained with an increased number of beams. Findings can be compared to results in the literature that are designed according to provisions of other countries' standards. Obtained results can be also supported by numerical studies.

Acknowledgments

This research was supported by the Muğla Sıtkı Koçman University Scientific Research Projects (Project No: 15-007). The authors of this experimental study wish to express their

grateful acknowledgment of financial support. Also, steel fiber used in this study was supplied from Kemerli Metal Pty Ltd., Turkey. We are thankful for the procurement of steel fibers.

References

[1] Ersoy, U., Winter, G., Nilson, A. H., Design of Concrete Structures, 11th ed., McGraw-Hill, New York. 1999

[2] Hsu, T. T. Torsion of structural concrete-behavior of reinforced concrete rectangular members. Special Publication, 18, 261-306, 1968.

[3] Ju, H., Lee, D., Kim, J.R., Kim, K.S., Maximum torsional reinforcement ratio of reinforced concrete beams, Structures, 23, 481–493, 2020. https://doi.org/10.1016/j.istruc.2019.09.007

[4] Teixeira, M. M., Bernardo, L., Ductility of RC beams under torsion, Engineering Structures, 168, 759-769, 2018.. https://doi.org/10.1016/j.engstruct.2018.05.021

[5] Narayanan, R., Kareem-Palanjian, A. S., Torsion in beams reinforced with bars and fibers, Journal of Structural Engineering, 112(1), 53-66, 1968. https://doi.org/10.1061/(ASCE)0733-9445(1986)112:1(53)

[6] Kim, M.J., Kim H.G., Lee, Y.J., Kim, D.H., Lee, J.Y., Kim, H.E., Pure torsional behavior of RC beams in relation to the amount of torsional reinforcement and cross-sectional properties, Construction and Building Materials 260, 119801, 2020. https://doi.org/10.1016/j.conbuildmat.2020.119801

[7] Rasmussen, L., Baker, G., Torsion in reinforced normal and high-strength concrete beams part 1: Experimental test series, ACI Structural Journal, 92(1), 56-62, 1995.

[8] Waryosh, W. A., Mohaisen, S. K., Dkhel, R. H., Experimental study on torsional behavior of fiberious reinforced concrete beams with different concrete strength, IOP Conference Series: Materials Science and Engineering, 584, 2019. https://doi:10.1088/1757-899X/584/1/012052

[9] Kaya, S. Yalcin, C., Kaya, O. Experimental investigation of full-scale reinforced concrete beams under reversed-cyclic pure torsion, Structures, 51, 734-746, 2023. https://doi.org/10.1016/j.istruc.2023.03.079

[10] Facconi, L., Minelli, F., Ceresa, P, Plizzari, G. Steel fibers for replacing minimum reinforcement in beams under torsion, Materials and Structures, 54, 2021. https://doi.org/10.1617/s11527-021-01615-y

[11] Cucchiara, C., Mendola, L., Papia, M., Effectiveness of stirrups and steel fibres as shear reinforcement, Cement and Concrete Composites, 26(7), 777-786 2004. https://doi.org/10.1016/j.cemconcomp.2003.07.001

[12] Craig, R. J., Parr, J. A., Germain, E., Mosquera, V., Kamilares, S., Fiber reinforced beams in torsion, Journal Proceedings, 83(6), 934-942, 1986.

[13] Engin, S., Ozturk, O., Okay, F., Estimation of ultimate torque capacity of the SFRC beams using ANN, Structural Engineering and Mechanics, 53(5), 939-956, 2015. https://doi.org/10.12989/sem.2015.53.5.939

[14] Rao, T. G., Seshu, D. R., Torsion of steel fiber reinforced concrete members, Cement and Concrete Research, 33(11), 1783-1788, 2003. https://doi.org/10.1016/S0008-8846(03)00174-1

[15] Yang, I.-H., Joh, C., Lee, J. W., Kim, B.-S., Torsional behavior of ultra-high performance concrete squared beams, Engineering Structures, 56, 372-383, 2013. https://doi.org/10.1016/j.engstruct.2013.05.027

[16] Anandan, S., Effect of Steel fibre profile on the fracture characteristics of steel fibre reinforced concrete beams, Journal of Engineering Research, 7(2), 105-124, 2019

[17] Mansur, M. A., Nagataki, S., Lee, S. H., Oosumimoto, Y., Torsional response of fibrous concrete beams, ACI Structural Journal, 86(1), 36-44, 1989.

[18] Okay, F., Engin, S., Torsional behavior of steel fiber reinforced concrete beams, Construction and Building Materials, 28(1), 269-275. 2012. https://doi.org/10.1016/j.conbuildmat.2011.08.062

[19] Kamiski, M., Pawlak, W., Load capacity and stiffness of angular cross section reinforced concrete beams under torsion, Archives of Civil and Mechanical Engineering, 11(4), 885–903, 2011. https://doi.org/10.1016/s1644-9665(12)60085-5

[20] Salama, A.E., Kassem, M.E., Mahmoud, A.A., Torsional behavior of T- shaped reinforced concrete beams with large web openings, Journal of Building Engineering 18, 84-94, 2018. https://doi.org/10.1016/j.jobe.2018.02.004

[21] Chalioris, C. E., Karayinnis, C. G., Effectiveness of the use of steel fibers on the torsional behavior flanged concrete beams, Cement and Concrete Composites 31(5), 331-341, 2009 https://doi.org/10.1016/j.cemconcomp.2009.02.007

[22] ACI Committee 318. Building code requirements for reinforced concrete and commentary (ACI 318-14). American Concrete Institute, Detroit, MI, 2014.

[23] Comete European de Normalisation (CEN), Eurocode 2: design of concrete structures. Part 1-general rules and rules for buildings, pr EN 1992-1, 225, 2004.

[24] CSA Committee A23.3-14, Design of Concrete Structures (CAN/CSA-A23.3-14), Canadian Standards Association, Canada, 297, 2014.

[25] Japan Society of Civil Engineering, Standard Specifications for Concrete Structures, Japan Society of Civil Engineering, Japan, 2007.

[26] Amin, A., Bentz, E. C., Strength of steel fiber reinforced concrete beams in pure torsion, Structural Concrete, 19(3), 684-694, 2018. https://doi.org/10.1002/suco.201700183

[27] Ilkhani, M.H., Naderpour, H., Kheyroddin, A., A proposed novel approach for torsional strength prediction of RC beams, Journal of Building Engineering, 25, 2019. https://doi.org/10.1016/j.jobe.2019.100810

[28] Oettel, V. Steel fiber reinforced RC beams in pure torsion—Load-bearing behavior and modified space truss model, Structural Concrete, 24(1), 1348-1363, 2023. https://doi.org/10.1002/suco.202200031

[29] Kryzhanovskiy, K., Zhang, D., Ju, H. et al. Development of Torsional Strength Model for Steel Fiber Reinforced Concrete Beams with Transverse Reinforcement. Int J Civ Eng 21, 1123–1139, 2023. https://doi.org/10.1007/s40999-023-00816-6

[30] Turkish Standard TS500, Requirements for Design and Construction of Reinforced Concrete Structures. Turkish Standards Institution, Ankara, Turkey, 2000.

[31] Raut, L.L., Kulkarni, D.B., Torsional strengthening of under reinforced concrete beams using crimped steel fiber, International Journal of Research in Engineering and Technology 3(6), 2014. https://doi.org/10.15623/ijret.2014.0306087

[32] Narayanan, R., Darwish, I. S., Use of steel fibers as shear reinforcement, ACI Structural Journal 84(3), 216-27. 1987.

[33] Chalioris, C. E., Steel fibrous RC beams subjected to cyclic deformations under predominant shear, Engineering Structures, 49, 104-118, 2013. https://doi.org/10.1016/j.engstruct.2012.10.010

[34] Ju, H., Lee, D. H., Kim, K. S., Minimum torsional reinforcement ratio for reinforced concrete members with steel fibers, Composite Structures, 207, 460-470, 2019 https://doi.org/10.1016/j.compstruct.2018.09.068

[35] Naaman, A. E., Engineered steel fibers with optimal properties for reinforcement of cement composites, Journal of Advanced Concrete Technology, 1(3), 241-252, 2003. https://doi.org/10.3151/jact.1.241

[36] Hameed, A. A., Al-Sherrawi, M. H., Torsional strength of steel fiber reinforced concrete beams, International Journal of Civil Engineering and Technology 9(6), 1388–1396, 2018.

[37] Hanoon, A. N., Abdulhameed, A. A., Abdulhameed, H. A., Mohaisen, S. K., Energy absorption evaluation of CFRP-strengthened two-spans reinforced concrete beams under pure torsion, Civil Engineering Journal, 5(9), 2007-2018. 2019. http://dx.doi.org/10.28991/cej-2019-03091389

[38] Patil, S. P., Sangle, K. K., Tests of steel fiber reinforced concrete beams under predominant torsion, Journal of Building Engineering 6, 157-162, 2016. https://doi.org/10.1016/j.jobe.2016.02.004

[39] Ju, H., Han, S.-J., Zhang, D., Kim, J., Wu, W., Kim, K. S., Estimation of minimum torsional reinforcement of reinforced concrete members, Advances in Materials Science and Engineering, 1-10, 2019. https://doi.org/10.1155/2019/4595363